

Density functional analysis of conducting molecules: A Theoretical Investigation via QTAIM approach

P. Jayalakshmi^{1,a}, B. Jothi^a, K. Selvaraju^a, A. David Stephen^b

^aDepartment of Physics, Kandaswami Kandaru's College, Velur 638182 Tamilnadu, India.

^bDepartment of Physics, PSG College of Arts and Science, Coimbatore 641014 Tamilnadu, India.

Abstract: The assessment of quaterphenyl and quarter (1,4 dithiine) molecules joining the spatial dissemination of electron inside the framework, was finished using Density Functional analysis incorporated with LANL2DZ premise set joined with the Bader's AIM theory. All the examinations were carried out within growing electric field from 0.05–0.26VÅ⁻¹. The chemical nature and the topological assessment of the nano wire were studied in detail by subjecting the same to external electric field to prove the possible commercial importance of the structure in the field of nanoelectronics. HOMO-LUMO assessment was made to choose the way in which the one-dimensional nanowires show conductivity. The I-V characteristic plot and ESP surface were generated to study the conducting nature of the nanowires.

Keywords: QTAIM, Molecular orbital, Electrostatic potential, Conductivity, Bandgap.

1. Introduction

The developments in molecular design have made it possible to tune the molecular structures of organic semiconductors to meet the industrial necessities for manufacturing practical devices. Designing of novel device configurations is becoming more critical because rationalizing of molecular electronic component is reaching a perilous limit. The use of nanowires is a probable substitute to conventional diodes and transistors.[1]. As the nanoscale materials have many applications in various industries, many efforts been undertaken to find the electrical conductivity in nanowires. However, there was the limited success met by the researchers in establishing the flexible nano scale conductors due to the challenges associated with the property changes with the applied voltages. Recent years, considerable researches focus the variation of structural and electron transport properties of many molecules [2-3].

In the present study, the electrical conductivity of quaterphenyl and quarter (1,4 dithiine molecular nanowires [hereafter it is referred as molecule I and molecule II] were studied (Figure 1). The variations in geometrical parameters of the molecule I and II were analyzed with zero bias to higher electric fields (EFs). The charge density and total energy density of the molecules for various EFs describe the geometrical conformation of both the molecules. The molecular orbital analysis, variation in electrostatic potentials, molecular dipole moment and the current–voltage characteristics provide an interesting information to analyze new molecular nanowires.

2. Computational Method

The molecules I and II has been optimized from zero to ±0.26 VÅ⁻¹ using density functional theory incorporated in Gaussian09 program package [4].

¹ Corresponding Author

e-mail: manijaya2003@gmail.com

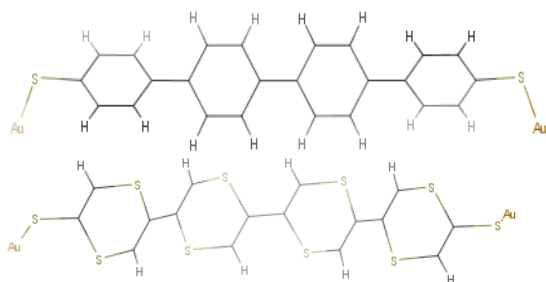


Figure 1. Schematic diagram of molecule I and II fused with Sulphur and Gold atoms.

For the optimization, permutation of Becke's three-parameter exchange function with B3LYP hybrid function [5] is used along with LANL2DZ [6] basis set as it delivers the complete explanation of heavy metal atoms in the molecular wire. The Mulliken population analysis [MPA] charges [7] were calculated with polarization and diffuse functions. In this computation, the Van der Waals radius of gold and Sulphur atom has been encompassed in the input file.

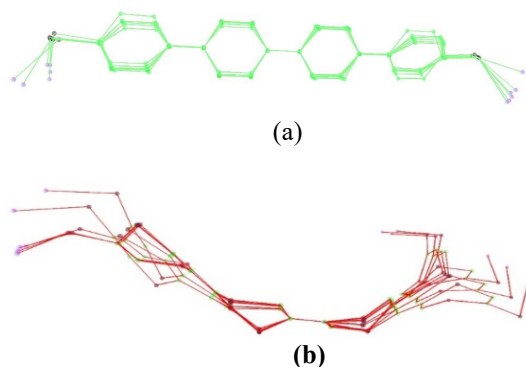


Figure 2. Superimpose of the Au & S substituted molecule I and II for the zero and various applied EFs.

The structural energy minimization was evaluated through Bery algorithm [8] and the optimization is converged with the required threshold values. In this study, all the quantum computation was carried out for different levels of external fields to analyze the variations in the geometry conformation, chemical bond characteristics and the ESP of the molecules I and II. The bond topological and the electrostatic properties have been predicted from the quantum theory of atoms in molecules [QTAIM] theory [9] via EXT94b module implemented in the AIMPAC software [10]. DENPROP combined with wfn2plots generated two dimensional grids for mapping the Laplacian of electron density and the deformation density. The gaussian visualizing package GVVIEW was used to

explore the three-dimensional surface plots. The density of states (DOS) for different applied EFs was well framed from the GaussSum program [11].

3. Results and discussion

3.1 Structural aspect

The superposition of I and II molecular wires with different external fields were shown in Figure 2 (a & b) from which it was observed that the geometry of the molecule I is not changing significantly with the applied electric field from 0 to 0.26 V/Å. On contrary, the application of different electric field to the molecule II affects the geometry. The supplementary table 1 displays the variation occurs in the bond length of both the molecule for the different external fields. The average C-C bond lengths of I in all the three six membered ring is ~1.411 Å, and the respective bond length is slightly stretched by 0.06 Å for molecule II, and this deviation attributes the presence of Sulphur atoms in the rings. On contrary, the average value of C-C bonds in between the six membered rings of I is 1.485 Å which is slightly elongated when compared with that of II, as its average value is 1.474 Å. With the application of the electric field increased from 0 to 0.26 V/Å, the C-S bond lengths in the three six membered rings varies with the maximum difference of 0.02 Å and its mean value is ~1.840 Å. The average Au-S bond distance in left/right closures of I and II molecules are 2.395 Å /2.425 Å and 2.406 Å /2.425 Å respectively. As molecule II is having Sulphur replacement in six membered rings, the dihedral angle is varied drastically when compared with that of I molecule.

3.2 QTAIM analysis

The electron density analysis and their topological properties were characterized with QTAIM theory proven by Bader (Bader, 1991). For the various fields, the 2D contour plots posing the dynamic deformation density in the molecular plane was exhibited from the Figure 3. The Laplacian of electron density [$\nabla^2 \rho_{bcp}(r)$], has been raised from second order partial derivative of electron density, which quantifies the curvature of the function in 3D. The negative value of Laplacian directs to the locally concentrated charges at the bcp and a positive value lead to the locally depleted. The 2D contour plot of Laplacian of electron density plotted

for the molecular plane was shown in the Figure 4. To investigate the bond strength, the total energy density $H(\mathbf{r})$ of the molecule has been examined. Table 1-3 list the electrical characteristics of both molecules. The positive Laplacian of electron density results the influence of the kinetic energy density, which leads the exhaustion of bond charge at the bond critical point; whereas the negative Laplacian represents the governance of potential energy density, and the concentration of charges. The total energy density $H(\mathbf{r})$ from potential energy density $V(\mathbf{r})$ and the local kinetic energy density $G(\mathbf{r})$ in the bonding region can be equated as $H(\mathbf{r}) = G(\mathbf{r}) + V(\mathbf{r})$. The current study reports that the $G(\mathbf{r})$ is positive, $V(\mathbf{r})$ is negative and $H(\mathbf{r})$ is negative, it is obvious that $V(\mathbf{r})$ is always leads in all cases. The average value of $\rho_{\text{bcp}}(\mathbf{r})$ for aromatic C-C bonds is calculated for molecule I is $1.89 \text{ e}/\text{\AA}^3$ under zero bias condition. When the two electrodes are subjected to $0.05 \text{ V}/\text{\AA}$, the electron density value in the bonding region is increased slightly to $1.92 \text{ e}/\text{\AA}^3$ and it is found to be stable for the maximum applied electric field $0.26 \text{ V}/\text{\AA}$. The Sulphur replacement in the six membered rings of molecule II makes high electron accumulation when compared to molecule I, and the $\rho_{\text{bcp}}(\mathbf{r})$ is $2.10 \text{ e}/\text{\AA}^3$ for zero bias, and there is no significant change due to external field. The covalent characteristic of C-C bonds in both molecule I/II was further confirmed from $[\nabla^2\rho_{\text{bcp}}(\mathbf{r})]$ and $[H(\mathbf{r})]$ at the bond critical point, the corresponding values are $\sim -17.8 \text{ e}\text{\AA}^{-5}/\sim -20.4 \text{ e}\text{\AA}^{-5}$ and $\sim -1.88 \text{ H}\text{\AA}^{-3}/\sim -2.13 \text{ H}\text{\AA}^{-3}$ respectively. This slight variation of the topology values of I and II attributes the presence of Sulphur atoms in the six membered rings. The characteristics of chemical bonding between carbon and thiol atoms in the six membered ring is well understood from their $\rho_{\text{bcp}}(\mathbf{r})$ and $\nabla^2\rho_{\text{bcp}}(\mathbf{r})$ values; $\sim 1.01 \text{ e}\text{\AA}^{-3}$ and $\sim -4.0 \text{ e}\text{\AA}^{-5}$ respectively. The ionic bond characteristic of terminal C-S bonds of molecule I were evidenced from their bond topology values $1.02 \text{ e}\text{\AA}^{-3}$ [$\rho_{\text{bcp}}(\mathbf{r})$], $-4.2 \text{ e}\text{\AA}^{-5}$ [$\nabla^2\rho_{\text{bcp}}(\mathbf{r})$] and $-0.62 \text{ H}\text{\AA}^{-3}$ [$H(\mathbf{r})$] under zero bias situation, as the electric field increases from $0.05 \text{ V}/\text{\AA}$ to $0.26 \text{ V}/\text{\AA}$, these values undergo a slight change of around ~ 0.02 units in each head. The similar trend was noticed in the molecule II for the terminal C-S bonds. The *closed-shell* type Au-S interaction was evident from the positive values of Laplacian, $2.9 \text{ e}\text{\AA}^{-5}$ and $3.0 \text{ e}\text{\AA}^{-5}$ for left and right

end of the molecule I. Supplementary, it is observed that the charges of these bonds are well exhausted for the aggregated electric field, this charge delocalization can be envisaged from the Laplacian of electron density two-dimensional contour plots (Figure 4). The Laplacian of electron density values of Au-S bond in the left region differs from 2.9 to $3.5 \text{ e}\text{\AA}^{-5}$, whereas in the right region, there is no significant variation was found for higher field [$0 - 0.26 \text{ V}\text{\AA}^{-1}$]. Similar pattern was observed for II molecule. As expected, the minimum total energy density $H(\mathbf{r})$ is found for Au-S bonds, as their average value is $\sim -0.15 \text{ H}\text{\AA}^{-3}$.

3.3. Electrostatic Potential

Gadre and co-workers [12] reported earlier that the topography plotting of iso-surface of the electrostatic potential (ESP) is a succinct way to investigate the molecule to study the chemical reactivity and electrostatic property. One of the major works of the present study is the molecular electrostatic potential (MESP) resulted from the charge distribution which allows to locate the high electronegative and electropositive regions [13-16]. Figure.5 displays the three-dimensional iso surface representations of electrostatic potential for the molecules I and II under zero and non-zero bias. Here, blue region denotes positive potential and red region symbolizes negative potential. The surface potential obviously replicates the opposing influences from the nuclei and the electrons, therefore it highly portraited the charged sections of the molecule.

The surface is found to be positive all over the molecular backbone for the zero various fields; this positive influence is qualified from the nuclei. While, the negative potential is pivoted over Sulphur atoms present at both ends of the molecule; this situation is nearly even when the field gets escalated from 0 to $0.15 \text{ V}\text{\AA}^{-1}$. When the field is increased further to $0.21 \text{ V}\text{\AA}^{-1}$, the negative electrostatic potential was found to be mounted at the left edge, which gets diluted to a smaller value at $0.26 \text{ V}\text{\AA}^{-1}$.

Further, the balance parameter [12] was calculated for molecules I and II to explicit the exact composition of positive and negative potential. The balance parameter reaches a maximum value 0.25 ,

when $\sigma^2(+)=\sigma^2(-)$. The calculated MSEP variances with balance parameter are listed in table 4 and the variation of balance parameter with the electric fields are shown in the Figure 6.

Table 1 (a). Electron density $\rho_{bcp}(r)$ ($e\text{\AA}^{-3}$) values for the terminal bonds of the molecule I for the various applied EFs ($V\text{\AA}^{-1}$).

Bonds	0	0.05	0.10	0.16	0.21	0.26
S(43)-C(34)	1.018	1.022	1.027	1.033	1.035	1.035
C(1)-S(41)	1.018	1.015	1.012	1.011	1.037	1.054
S(41)-Au(42)	0.52	0.522	0.523	0.524	0.539	0.537
S(43)-Au(44)	0.52	0.517	0.513	0.506	0.479	0.456

Table 1 (b). Electron density $\rho_{bcp}(r)$ ($e\text{\AA}^{-3}$) values for the terminal bonds of the molecule II for the various applied EFs ($V\text{\AA}^{-1}$).

Bonds	0	0.05	0.10	0.16	0.21	0.26
C(1)-S(25)	1.023	1.022	1.021	1.019	1.012	1.014
S(27)-C(21)	1.021	1.023	1.023	1.019	1.022	1.019
Au(28)-S(27)	0.516	0.514	0.515	0.517	0.485	0.457
S(25)-Au(26)	0.517	0.517	0.519	0.521	0.517	0.513

Table 2 (a). Laplacian of electron density values for the terminal bonds of the molecule I for the various applied EFs ($V\text{\AA}^{-1}$).

Bonds	0	0.05	0.10	0.16	0.21	0.26
S(43)-C(34)	-4.213	-4.254	-4.311	-4.394	-4.442	-4.469
C(1)-S(41)	-4.211	-4.181	-4.16	-4.152	-4.517	-4.787
S(41)-Au(42)	2.927	2.955	2.987	3.027	3.318	3.453
S(43)-Au(44)	2.927	2.902	2.883	2.878	2.949	2.981

Table 2 (b). Laplacian of electron density values for the terminal bonds of the molecule II for the various applied EFs ($V\text{\AA}^{-1}$).

Bonds	0	0.05	0.10	0.16	0.21	0.26
C(1)-S(25)	-4.349	-4.359	-4.369	-4.366	-4.332	-4.517
S(27)-C(21)	-4.324	-4.328	-4.304	-4.231	-4.34	-4.336
Au(28)-S(27)	3.031	3.11	3.117	3.121	3.055	3.097
S(25)-Au(26)	3.113	3.141	3.176	3.222	3.232	3.328

Table 3 (a). Total energy density $H(r)$ ($H\text{\AA}^{-3}$) values for the terminal bonds of the molecule I for the various applied EFs ($V\text{\AA}^{-1}$).

Bonds	0	0.05	0.10	0.16	0.21	0.26
S(43)-C(34)	-0.618	-0.622	-0.627	-0.637	-0.646	-0.654
C(1)-S(41)	-0.618	-0.616	-0.615	-0.617	-0.654	-0.683
S(41)-Au(42)	-0.156	-0.157	-0.157	-0.157	-0.163	-0.16
S(43)-Au(44)	-0.156	-0.155	-0.152	-0.148	-0.133	-0.119

Table 3 (b). Total energy density $H(r)$ ($H\text{\AA}^{-3}$) values for the terminal bonds of the molecule II for the various applied EFs ($V\text{\AA}^{-1}$).

Bonds	0	0.05	0.10	0.16	0.21	0.26
C(1)-S(25)	-0.668	-0.671	-0.675	-0.676	-0.677	-0.706
S(27)-C(21)	-0.663	-0.665	-0.663	-0.655	-0.665	-0.671
Au(28)-S(27)	-0.153	-0.151	-0.151	-0.152	-0.135	-0.118
S(25)-Au(26)	-0.152	-0.152	-0.152	-0.153	-0.15	-0.147

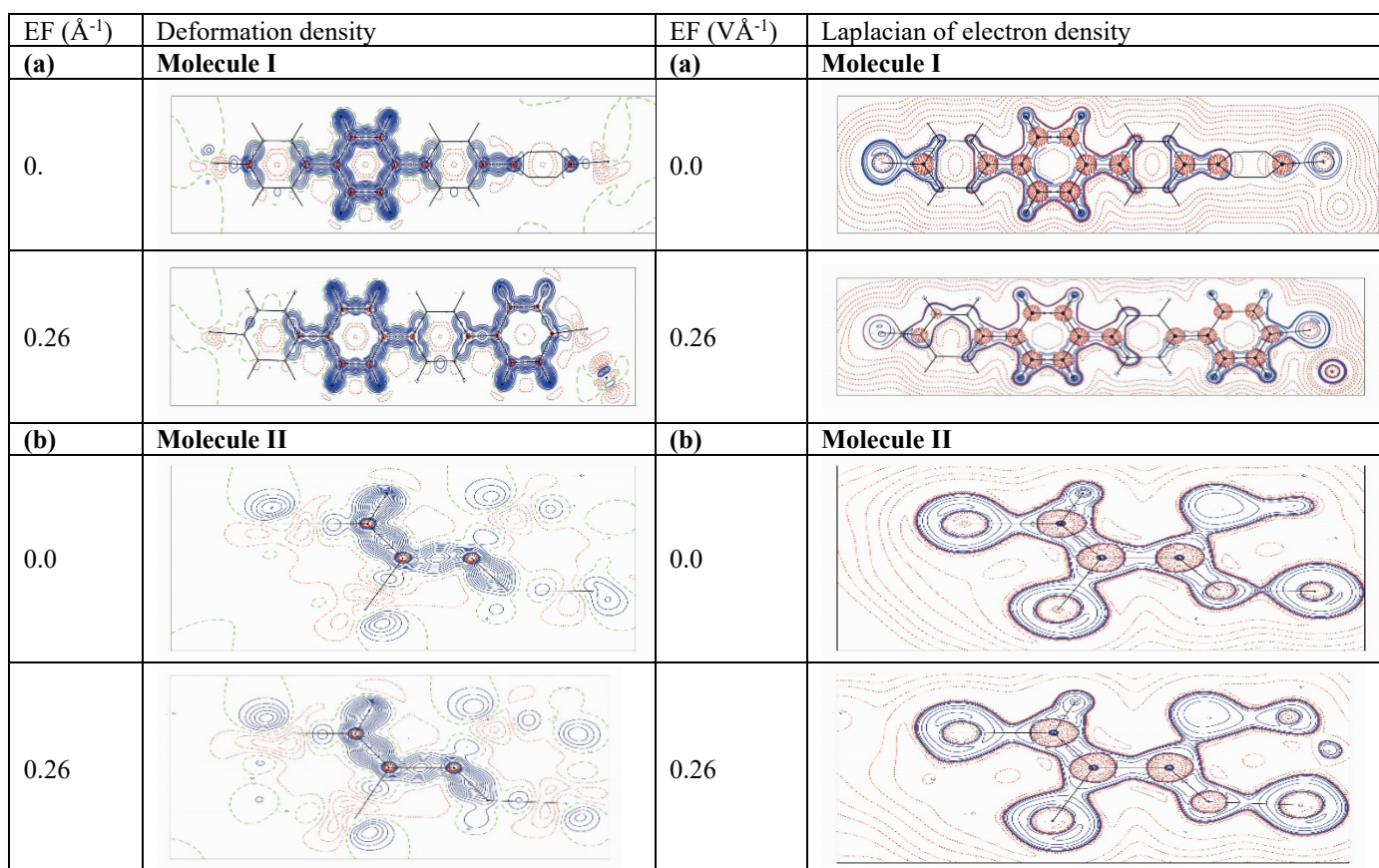


Figure 3. Deformation density map plotted for molecular plane of (a) molecule I and (b) molecule II for the zero and 0.26 applied EFs. Solid lines represent positive contours; dotted lines are negative contours and dashed lines are zero contours. The contours are drawn at $0.05 \text{ e}\text{\AA}^{-3}$ intervals.

Figure 4. Laplacian of electron density map plotted for molecular plane of (a) molecule I and (b) molecule II for the zero and 0.26 applied EFs. The contours are drawn in logarithmic scale, $3 \times 2^N \text{ e}\text{\AA}^{-5}$, where $N = 2, 4$ and 8×10^n , $n = -2, -1, 0, 1, 2$. Solid lines are positive contours and dotted lines are negative contours.

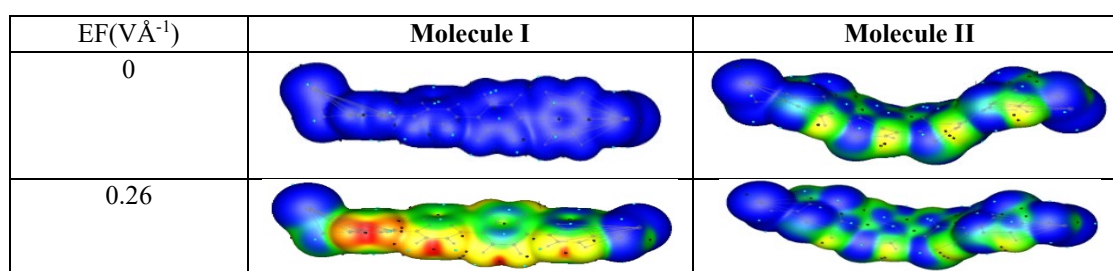


Figure 5. Isosurface representation of ESP of Au and S substituted I and II for EFs $0 \text{ V}\text{\AA}^{-1}$ and $0.26 \text{ V}\text{\AA}^{-1}$. Blue: positive potential ($0.5 \text{ e}\text{\AA}^{-1}$), Red: negative potential ($-0.04 \text{ e}\text{\AA}^{-1}$).

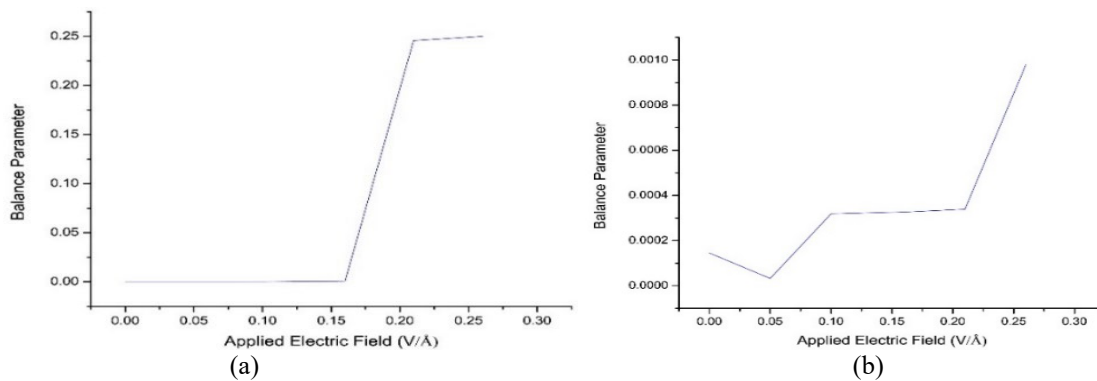


Figure 6. Variation of balance parameter for the zero and various applied EF of (a) molecule I and (b) molecule II

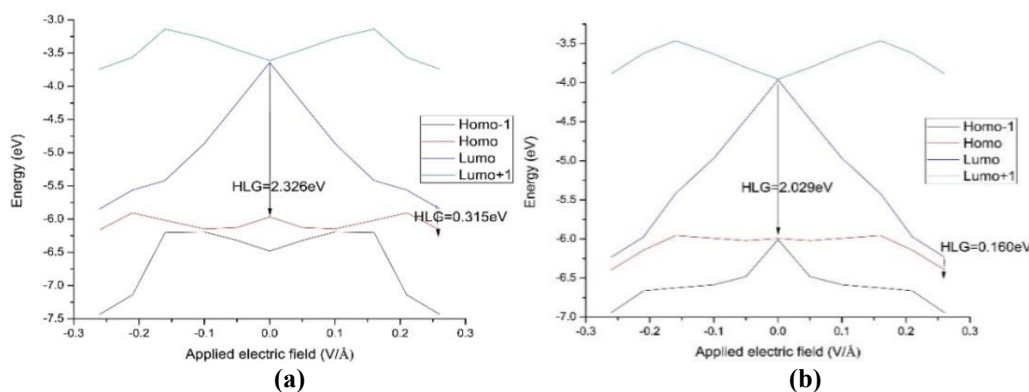


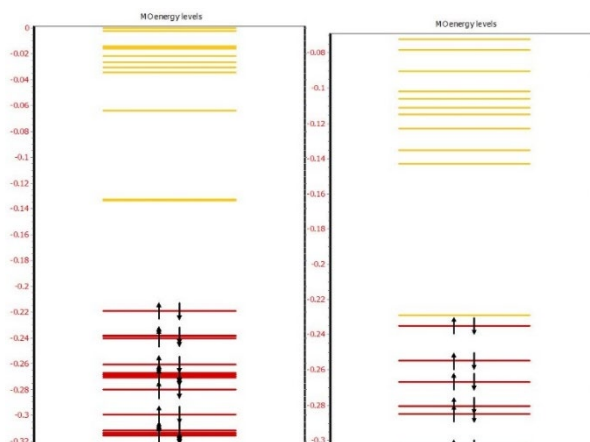
Figure 7. Variation of HLG for the various applied EFs in (a) molecule I and (b) molecule II.

Table 4 (a). Variance and balance parameter of Molecule I for various applied EFs.

EF(VÅ ⁻¹)	$\sigma^2(+)$	$\sigma^2(-)$	Balance parameter
0	2035834	24.8	0.00
0.05	2.41	0.00	0.00
0.10	0.74	0.00	0.00
0.16	0.16	0.00	0.00
0.21	0.00	0.00	0.25
0.26	230.98	236	0.25

Table 4 (b). Variance and balance parameter of the molecule II for various applied EFs,

EF(VÅ ⁻¹)	$\sigma^2(+)$	$\sigma^2(-)$	Balance parameter
0	165028.52	23.91	0.00
0.05	1.90	0.00	0.00
0.10	0.23	0.00	0.00
0.16	0.28	0.00	0.00
0.21	0.63	0.00	0.00
0.26	182839.89	179.37	0.00



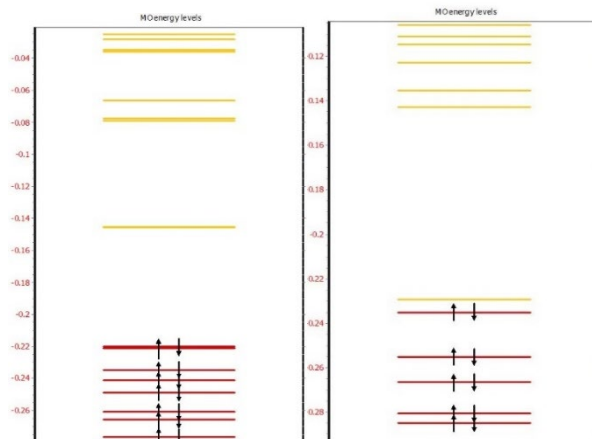


Figure 8. MO energy level of (a) molecule I and (b) molecule II (0 and 0.26 eV)

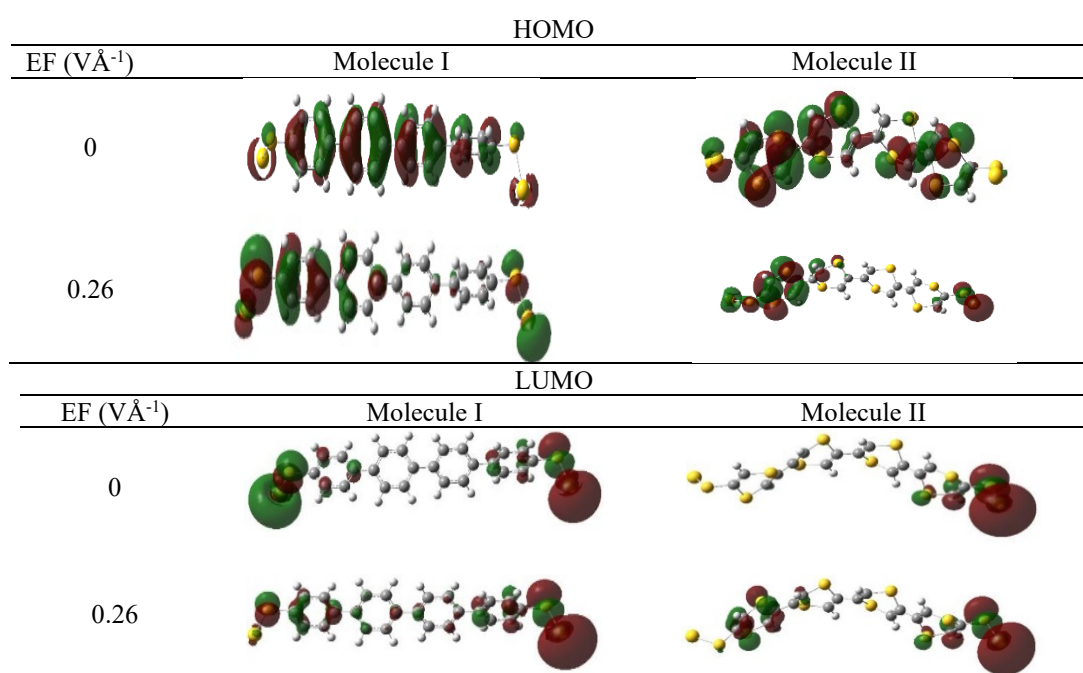


Figure 9. Iso surface representation of molecular orbitals (HOMO, LUMO) I and II for the zero and various applied EFs, which are drawn at 0.05au surface values.

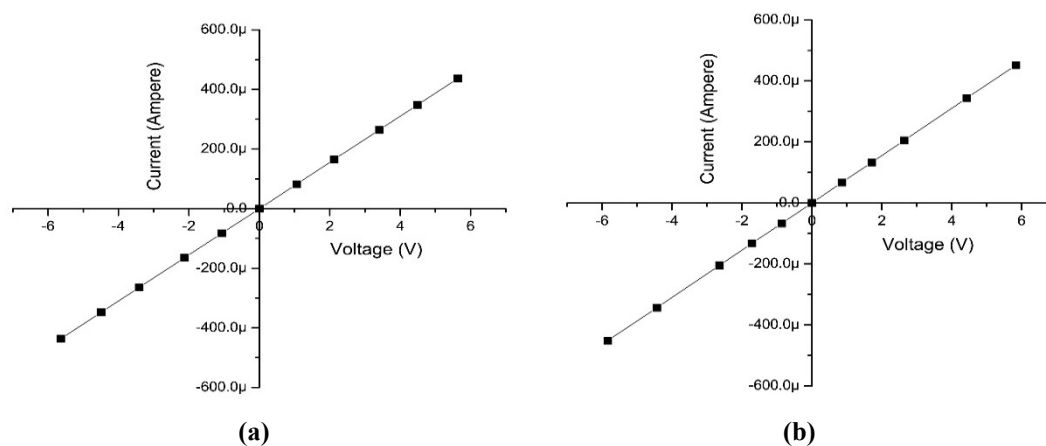


Figure 10. I-V characteristics plot of Au and S substituted (a) molecule I and (b) molecule II for the zero and various applied EF

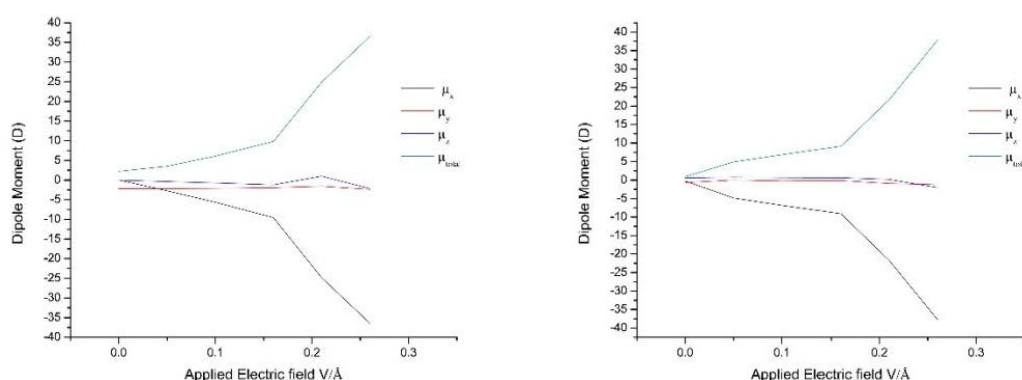


Figure 11. Molecular dipole moment of Au and S substituted molecule I and molecule II

3.4. Frontier Molecular orbital analysis

The HOMO-LUMO gap (HLG) of a molecule which directs the charge transport properties of the molecular nano wire [17-19]. Henceforth, it is vital to examine the alterations in HLG and molecular orbital energy levels for the external fields. Figure 7 depicts the variation of HLG for the zero and non-zero bias of molecular wire. The applied electric field significantly point out the frontier orbital energy levels of the system which are varied from each other and are predominantly symmetric for the reverse field effect. The external field made large differences in the distribution of orbital. As the molecules are subjected to the field from 0 to 0.26 $\text{V}\text{\AA}^{-1}$, there is sharp decrement in HOMO-LUMO gap from 2.326 to 0.315 eV for I and from 2.029 to 0.160 eV for molecule II Figure.7. The HOMO and LUMO levels and surfaces for 0 and 0.26 eV was shown in the Figures 8 and 9.

3.5. I-V relation and molecular polarization

The current-voltage (I-V) characteristic curve generally provides information to find the fundamental parameters of molecular electronic instruments [20]. The I-V characteristic plot Figure 10 of the gold and thiol substituted molecules I and II show that, the current increases gradually due to the increase of bias voltage showing almost linear ohmic character [21] (Kirtman et al., 2000). Polarization of the molecule takes place with the application of external fields, which varies the molecular dipole moment. Hence, it is essential to calculate the molecular dipole moment with external EFs. The molecule found to be highly polarized at

higher electric field. The Figure11 shows the values of molecular dipole moment μ_x , μ_y , and μ_z along x, y and z directions and μ represents the resultant molecular dipole moment for different external EFs. The application of field along x-direction may contribute the large variation of x-component.

4. Conclusion

The effect of the growing electric field over molecule I and molecule II were studied by implementing the higher order DFT calculations and QTAIM analysis. The result showed that the electric field affect vigorously over the geometry of the molecule II, while the molecule I showed negligible alterations. The investigation on the electron density and topological parameters in the varying electric field were studied by incorporating Quantum theory. The result indicated the steady nature of the chemical bonds by exhibiting insignificant variations in the electron density for the bonds in both wires. The results exposed the variation of the band gap energy for both nanowires as the field rises from zero to 0.26 $\text{V}\text{\AA}^{-1}$, the HOMO-LUMO gap of both nanowires reduced to 0.315 eV and 0.160 eV from a value of ~ 2 eV, indicating the accumulation of charges. I-V curves are generally employed as a device to decide and realize the essential boundaries of a segment or appliance and which can also be functioned to numerically show its behavior inside an electronic circuit. The I-V characteristic curve of the nanowires under study indicated linear behavior, where the current were proportional to voltage as in ideal

resistor. The property exposed the possibility of the applications of the concerned nanowires in electronic circuits.

References

- [1] W. Yutaka, H. Ryoma, C. Toyohiro, M. Shinichi, N. Tomonobu, E. Stefan, Dimas de O. Helmut D., and K. Kenji, Self-Assembled Molecular Nanowires of 6,13-Bis(methylthio)pentacene: Growth, Electrical Properties, and Applications. *Nano Letters*, 8 (10) (2008) 3273-7.
- [2] A. Irfan, J. Zhang, and Y. Chang, Theoretical investigations of the charge transfer properties of anthracene derivatives. *Theoretical Chemistry Accounts*, 137 (1) (2018) 1-15.
- [3] G. Erik, M. Liqiang and Y. Peidong Introduction: 1D Nanomaterials/Nanowires. *Chemical Reviews*, 119 (15) (2019) 8955–8957.
- [4] M.J. Frisch, Trucks., G.W. Schlegel, G.E. Scuseria, M.A. Robb, J.R. Cheeseman, G. Scalmani, V. Barone, B. Mennucci, et al., Gaussian09. In *Journal of the American Statistical Association*, (2009).
- [5] P. Geerlings, F. De Proft, and W. Langenaeker, Conceptual Density Functional Theory. *Chemical Reviews*, 103(5) (2003) 1793-873.
- [6] C.E. Check, T.O. Faust, J.M. Bailey, B.J. Wright, T.M. Gilbert, and L.S. Sunderlin, Addition of polarization and diffuse functions to the LANL2DZ basis set for P-block elements. *Journal of Physical Chemistry A*, 105 (2001) 8111.
- [7] R. Carbó-Dorca, and P. Bultinck, Quantum mechanical basis for Mulliken population analysis. *Journal of Mathematical Chemistry*, 6(3) (2004) 231- 239.
- [8] V. Suleimanov, and W.H. Green, Automated Discovery of Elementary Chemical Reaction Steps Using Freezing String and Berny Optimization Methods. *Journal of Chemical Theory and Computation*, 11(9) (2015) 4248-59.
- [9] A. Bader Quantum Theory of Molecular Structure and Its Applications. *Chemical Reviews*, 91 (1991) 893– 928.
- [10] AIM 2000 Journal of Computational Chemistry, 22 (2001) 545-559.
- [11] N.M. O’Boyle, A.L. Tenderholt, and K.M. Langner, Cclib: A library for package-independent computational chemistry algorithms. *Journal of Computational Chemistry*, 29 (2008) 839-845.
- [12] S.R. Gadre, R.K. Pathak, Nonexistence of local maxima in molecular electrostatic potential maps. *Proc. Indian Acad. Sci. - Chem. Sci*, 102 (2) (1990) 189-192.
- [13] J.S. Murray and P. Politzer, The electrostatic potential: An overview. *Wiley Interdisciplinary Reviews: Computational Molecular Science*, 1 (2011) 153-163.
- [14] R. Prakash Chandra, L. Frederick and L.V.Marcel Practical High-Quality Electrostatic Potential Surfaces for Drug Discovery Using a Graph-Convolutional Deep Neural Network. *Journal of Medicinal Chemistry*, 63 (16) (2020) 8778–8790.
- [15] E. Pettersen, T. Goddard, C. Huang, G. Couch, D. Greenblatt, E. Meng, and T. Ferrin, UCSF Chimera - A Visualization System for Exploratory Research and Analysis. *Journal of Computational Chemistry*, 25 (2004) 1605–1612.
- [16] J.S. Murray, P. Politzer, Statistical analysis of the molecular surface electrostatic potential: An approach to describing noncovalent interactions in condensed phases. *J. Mol. Struct. THEOCHEM*, 425 (1998) 107-114.
- [17] Z. Chamani, Z. Bayat, S.J. Mahdizadeh, Theoretical study of the electronic conduction through organic nanowires. *Journal of Structural Chemistry*, 55 (3) (2014) 530- 538.
- [18] S. Eliziane.Santos Vitória., S. ReisLuciana Guimarães Clebio, Nascimento Jr., Molecular wires formed from native and push-pull derivatives polypyrroles and β -cyclodextrins: A HOMO-LUMO gap theoretical investigation. *Chemical Physics Letters*, (730) (2019) 141-146.
- [19] G. Zhang, and C.B. Musgrave, Comparison of DFT methods for molecular orbital

eigenvalue calculations. *Journal of Physical Chemistry A*, 111 (2007) 1554–1561.

- [20] V. Mujica, M. A. Ratner, Current-voltage characteristics of tunneling molecular junctions for off-resonance injection. *Chemical Physics*, 264 (2001) 365-370.
- [21] B. Kirtman, B. Champagne, and D.M. Bishop, Electric field simulation of substituents in donor - Acceptor polyenes: A comparison with ab initio predictions for dipole moments, polarizabilities, and hyperpolarizabilities. *Journal of the American Chemical Society*, 122 (2000) 8007–8012.